



Visualizing Surface T-Cell Receptor Dynamics Four-Dimensionally Using Lattice Light-Sheet Microscopy

Jillian Rosenberg¹, Jun Huang^{1,2}

¹Committee on Cancer Biology, The University of Chicago

²Pritzker School of Molecular Engineering, The University of Chicago

Abstract

The signaling and function of a cell are dictated by the dynamic structures and interactions of its surface receptors. To truly understand the structure-function relationship of these receptors in situ, we need to visualize and track them on the live cell surface with enough spatiotemporal resolution. Here we show how to use recently developed Lattice Light-Sheet Microscopy (LLSM) to image T-cell receptors (TCRs) four-dimensionally (4D, space and time) at the live cell membrane. T cells are one of the main effector cells of the adaptive immune system, and here we used T cells as an example to show that the signaling and function of these cells are driven by the dynamics and interactions of the TCRs. LLSM allows for 4D imaging with unprecedented spatiotemporal resolution. This microscopy technique therefore can be generally applied to a wide array of surface or intracellular molecules of different cells in biology.

Keywords

Biochemistry; Issue 155; lattice light-sheet microscopy; immunology; T-cell receptor; imaging; tracking; dynamics

Introduction

The precise dynamics of molecules trafficking and diffusing on the three-dimensional cell surface in real time have been an enigma to solve. Microscopy has always been a balance of speed, sensitivity, and resolution; if any one or two are maximized, the third is minimized. Therefore, due to the small size and immense speed with which surface receptors move, tracking their dynamics has remained a major technological challenge to the field of cell biology. For example, many studies have been conducted using total internal reflection fluorescence (TIRF) microscopy^{1,2,3}, which has high temporal resolution, but can only image a very thin slice of the T-cell membrane (~100 nm), and therefore misses events happening farther away in the cell. These TIRF images also only showing a two-dimensional

Correspondence to: Jun Huang at huangjun@uchicago.edu.

Disclosures

The authors have nothing to disclose.

Video Link

The video component of this article can be found at <https://www.jove.com/video/59914/>

section of the cell. By contrast, super-resolution techniques, such as stochastic optical reconstruction microscopy (STORM)⁴, photoactivated localization microscopy (PALM)⁵, and stimulated emission depletion microscopy (STED)⁶, can overcome the Abbe diffraction limit of light. These techniques have high spatial resolution (~20 nm resolution)^{4,5,6,7}, but they often take many minutes to acquire a full two-dimensional (2D) or three-dimensional (3D) image, and therefore the temporal resolution is lost. In addition, techniques such as STORM and PALM that rely on blinking signals may have inaccuracies in counting^{8,9}. Electron microscopy has by far the highest resolution (up to 50 pm resolution)¹⁰; it can even be conducted three-dimensionally with focused ion beam scanning electron microscopy (FIB-SEM), resulting in up to 3 nm XY and 500 nm Z resolution¹¹. However, any form of electron microscopy requires harsh sample preparation and can only be conducted with fixed cells or tissues, eliminating the possibility of imaging live samples over time.

Techniques to obtain the high spatiotemporal resolution required to identify the dynamics of surface and intracellular molecules in live cells in their true physiological 3D nature is only being recently developed. One of these techniques is Lattice Light-Sheet Microscopy (LLSM)¹², which utilizes a structured light sheet to drastically lower photobleaching. Developed in 2014 by Nobel Laureate Eric Betzig, the high axial resolution, low photobleaching and background noise, and ability to simultaneously image hundreds of planes per field of view make LLS microscopes superior to widefield, TIRF and confocal microscopes^{12,13,14,15,16,17,18,19}. This four-dimensional (x, y, z and time) imaging technique, while still diffraction limited (~200 nm XYZ resolution), has incredible temporal resolution (we have achieved a frame rate of about 100 fps, resulting in a 3D reconstructed cell image with 0.85 seconds per frame) for 3D spatial acquisition.

LLSM can be generally used to track real-time dynamics of any molecules within any cell at the single-molecule and single-cell level, particularly those in highly motile cells such as immune cells. For example, we show here how to use LLSM to visualize T-cell receptor (TCR) dynamics. T cells are the effector cells of the adaptive immune system. TCRs are responsible for recognizing peptide-MHC (pMHC) ligands displayed on the surface of antigen-presenting cells (APC), which determines the selection, development, differentiation, fate, and function of a T cell. This recognition occurs at the interface between T cells and APCs, resulting in localized receptor clustering to form what is called the immunological synapse. While it is known that TCRs at the immunological synapse are imperative for T-cell effector function, still unknown are the underlying mechanisms of real-time TCR trafficking to the synapse. LLSM has allowed us to visualize in real time the dynamics of TCRs before and after trafficking to the synapse with the resultant pMHC-TCR interaction (Figure 1). LLSM can therefore be used to solve current questions of the formative dynamics of TCRs and provide insights to understand how a cell distinguishes between self and foreign antigens.

Protocol

5C.C7 TCR-transgenic RAG2 knockout mice in B10.A background were used in this study according to a protocol approved by the Institutional Animal Care and Use Committee of the University of Chicago.

1. Harvest and Activate T Cells—NOTE: This part of the protocol is based on previous protocols. See citations for further detail^{20,21}.

1. Euthanize a 10–12 week-old 5C.C7 transgenic mouse of either sex (~20–25 g) according to the approved IACUC protocol (i.e., CO₂ chamber followed by cervical dislocation).
2. Spray mouse carcass thoroughly with 70% ethanol to soak down the fur and bring into a BSL-2 safety cabinet.
3. Turn mouse onto its right side and make a small incision in the body cavity with surgical scissors. Remove the spleen using surgical forceps. Cut away connective tissue as needed with surgical scissors.
4. Place the spleen in a 70 µm-pore mesh cell strainer and mash with the back of a 1 mL syringe plunger. Wash through the strainer thoroughly with complete RPMI (RPMI with 10% fetal bovine serum [FBS], 2 mM L-glutamine, 1% penicillin/streptomycin, 50 µM 2-mercaptoethanol).
5. Centrifuge the single cell suspension of splenocytes at 300 × *g* for 5 min. Discard the supernatant.

NOTE: The pellet at this point will be red.

6. Resuspend the splenocytes in 5 mL RBC lysis buffer. Incubate for 5 min, then quench with 5 mL of complete RPMI.
7. Centrifuge the single cell suspension of splenocytes at 300 × *g* for 5 min. Discard the supernatant.

NOTE: The pellet at this point should be white, not red.

8. Resuspend the pellet in 5 mL of complete RPMI.
9. Transfer to a T-25 flask and add 10 µM moth cytochrome-C (MCC, sequence ANERADLIAYLKQATK). Put the cells in a cell culture incubator at 37 °C, 5% CO₂ overnight.
10. On the next day, add recombinant mouse IL-2 to a final concentration of 100 U/mL.
11. Observe for the following days, adding fresh media as the current media turns yellow. T cells will die if left in yellow media unattended for over 48 h. Cells are ready to use 6–10 days after harvest.

2. Prepare Cells

1. Incubate 5 mm round coverslips with 0.1% poly-L-lysine for 10 min. Aspirate off and let dry naturally.
2. Use a density gradient reagent (see the Table of Materials) to separate out dead cells and to obtain 1 × 10⁶ T cells and 1 × 10⁶ APCs (CH27 cells^{21,22} transduced with cytosolic mCherry) separately.

NOTE: Cells are counted using a hemocytometer.

1. Add 3 mL of density gradient reagent to a 15 mL conical tube and add cells dropwise to the edge of the tube carefully. **Do not mix.** Centrifuge at $930 \times g$ for 10 min at 4 °C; use acceleration/deceleration: SLOW/SLOW. Remove the thin middle layer of cells between the complete media and the density gradient reagent carefully, putting each cell type into separate conical tubes.

NOTE: It is necessary to prepare more cells than needed for imaging, as we find that 50% is lost on average during the process. The more cells used for the process, the easier it is to harvest them from the density gradient. We use 4–8 mL of both cell types to ensure excess cells. If desired, cells can be counted before this step to ensure volume needed. Any extra cells are put back into their respective flasks.

2. Wash both tubes of T cells and CH27 cells three times with 5 mL complete RPMI ($300 \times g$ for 5 min). Discard the supernatant each time during the wash. Resuspend each tube in 1 mL complete RPMI and count cells by a hemocytometer.
3. Resuspend 1×10^6 APCs in 500 μ L complete RPMI and add 10 μ M MCC. Incubate for 3 h at 37 °C, 5% CO₂. Wash cells three times with 500 μ L complete RPMI ($300 \times g$ for 5 min). Discard the supernatants.
4. Resuspend 1×10^6 T cells in 500 μ L complete RPMI. Add 2 μ g of anti-TCR β Alexa488-labeled Fab (clone H57) to 500 μ L of cells. Incubate for 30 min at 37 °C, 5% CO₂. Wash cells three times with 500 μ L of complete RPMI ($300 \times g$ for 5 min). Discard supernatant after each wash.

NOTE: The divalent anti-TCR antibody was cut into monovalent Fab using a Fab preparation kit (see the Table of Materials) to avoid crosslinking the T cell receptors by the divalent antibody (this step is optional).

5. Resuspend both cell types in 500 μ L of imaging media (phenol red-free Leibovitz's L-15 medium with 10% FBS, 1% penicillin/streptomycin, 2 mM L-glutamine).

3. Conducting LLSM Daily Alignment—NOTE: (Important) This alignment protocol is based on the LLSM instrument used (see the Table of Materials). Each LLSM may be different and require different alignment strategies, especially those that are home-built. Carry out the appropriate routine alignment and continue to section 4.

1. Add 10 mL of water plus 30 μ L fluorescein (1 mg/mL stock) to the LLSM bath (~10 mL volume), press Image (Home) to move the objective to image position, and look at a single Bessel laser beam pattern. Align the laser beam using the guides and pre-set region of interest (ROI) to make the beam a thin pattern balanced in all directions.

1. The beam should also appear focused in the finder camera. Use two mirror tilt adjusters, top micrometer, focus, and emission objective collar to adjust. See Figure 2A,B for correctly aligned beam.
2. Wash the bath and objectives with at least 200 mL of water to completely remove fluorescein.
3. Image standard fluorescent beads in the imaging media (prepared by adhering beads to a 5 mm coverslip with poly-L-lysine, see the Table of Materials; this can be pre-prepared and re-used) for physical point spread function (PSF) in imaging media.

NOTE: There can only be one bead in view for later processing, so try to find a bead that is by itself in the viewer or can easily be cropped to obtain a single bead.

1. Turn on **dither** by setting to 3 in the ‘X Galvo range’ box. Press **Live** to view the current field. Move along the Z direction to find the cover slip and beads. Find the center of a bead by moving along Z, press **Stop** to pause the laser. Check **3D**, press **Center** and then press **Execute**. This will collect the data.
2. Manually adjust the tilt mirror, objective collar, and focus micrometer for highest gray values, then adjust as necessary to obtain proper patterns for objective scan, z galvo, z+objective (totPSF), and sample scan (samplePSF) capture modes. See Figure 2C–F for properly adjusted maximum intensity projections (MIPs).

NOTE: The various captures modes (objective scan, z galvo, z +objective, and sample scan) change how the light-sheet moves through the sample. All scan modes should be used for alignment.

3. The sample scan shows how data will be collected during the experiment. Collect the sample PSF by pressing **Execute** in sample scan mode for deskewing and deconvolution (see section 5). Change lasers to three color mode (488, 560, 647) and press **Execute** again.

NOTE: Since the LLSM images at an angle (57.2°), images captured in the “sample scan” mode are collected at this angle, and are therefore “skewed”. De-skewing is the process of correcting for this angle and “re-aligning” the image to a true z-stack. These data **must** be collected in imaging media and in all channels that will be imaged during the experiment. If this is not collected properly, the data will not be properly de-skewed. Similarly, make sure media has been warmed to 37°C (or desired experimental temperature).

4. Setting Up Cells with LLSM

1. Add 100,000 APCs ($50\ \mu\text{L}$) from step 2.5 to a 5 mm-diameter circular coverslip from step 2.1 and allow them to settle for 10 min.

2. Grease the sample holder then add the coverslip cell-side-up to it. Add a drop of imaging media to the back of the coverslip to avoid bubbles before placing in the bath. Screw the sample holder onto the piezo, and press **Image (Home)**.
3. Find an APC to image to ensure that the LLSM and imaging software (see Table of Materials) are functioning properly.

NOTE: We image at 0.4 μm step size with 60 z-steps and 10 ms exposure for two colors with dither set to 3, which results in 1.54 s per frame of 3D image with ~ 200 nm XY and 400 nm Z resolution. These settings may need to be adjusted based on cell size, desired z-resolution, and strength of signal from the fluorescent labeling technique used. Laser power usage will also vary based on fluorescent labeling technique used.

1. Press **Live** to view the current image. Move along Z to find the cover slip and cells.
2. Find the center of an APC by moving in the Z direction, then press **Stop** to pause the laser. Check **3D** and input the desired settings (see step 4.3.1), press **Center** and then press **Execute**. This will collect the data.
4. Lower the stage to **load** position and add 50 μL of T cells in imaging media (100,000 cells, from step 2.5) dropwise directly over the coverslip. It is best to let a drop form on the end of the pipette tip and then touch the tip to the bath liquid. Raise stage back by clicking "**Image (Return)**".
5. Begin imaging. Be sure to set the desired stack size and time lapse length. For example, image 60 z-stacks at a 0.4 μm step size and input 500 time frames. (Typically) stop recording before 500 frames are reached to avoid photobleaching. Use **Live** mode to search for cell pairs, and when ready and desired settings have been entered, press **Execute** to collect data. See Movie 1 and Figure 1 for an example.

5. Track Surface Dynamics

1. Export the data from the imaging software (see the Table of Materials). This will create z-stack TIF files for every time point in each color.
2. First deskew and deconvolve the data.

NOTE: We use the LLSpy pipeline under license by HHMI's Janelia Research Campus¹⁸, but deskewing and deconvolution are also available within multiple imaging softwares (see Table of Materials).

3. Debleach the data.

NOTE: We use Fiji's debleach feature with histogram matching (Fiji Pathway: **Image | Adjust | Bleach Correction | Histogram Matching | OK**).
4. Import into the tracking software (see the Table of Materials). Track clusters according to software specifications. See Movie 2 for an example.

NOTE: Tracking results will depend upon the tracking software used, algorithm chosen, desired output parameters selected, etc. For example, in the tracking software we utilized (see the Table of Materials), we chose to allow the software to track irregular shapes, rather than assigning each feature a single spot, since TCR clusters are not organized into perfect spheres. In addition, we chose to collect 35 parameters, including speed, direction, volume, intensity, area, location, and track duration information. However, different methods or parameters will be beneficial to answer different questions.

1. If tracking is not desired, use the ClearVolume plugin for Fiji for visualizing and creating movies from hyperstack data.

Representative Results

Here, we describe the isolation, preparation, and imaging of primary mouse 5C.C7 T cells using a lattice light-sheet microscope. During section 3, it is imperative to align the microscope correctly, and to collect PSF daily with which to deconvolve the data after collection. In Figure 2, we show the correct alignment images that will be seen when aligning the microscope. Figure 2A and Figure 2B show the correct beam path and beam alignment, respectively, when imaged in fluorescein. The objective scan should show a large X shape in the XZ and YZ projections that is as symmetrical as possible; this should also be adjusted to be as small of an X as possible (Figure 2C). This is mainly achieved by adjusting the emission objective collar. The z galvo scan should show an oval in XZ and XY with a single dot on either side (above and below for XZ and to the left and right for YZ) (Figure 2D). This is mainly achieved by adjusting the galvo mirror tilt, either manually or with the motorized adjustment in the software. Finally, both the z+objective scan and the sample scan should show dots that look as round as possible (Figure 2E and Figure 2F, respectively). These may have a small X, but this should be as diminished as possible. These should be well aligned if the objective scan and z galvo were set well, but if adjustments are necessary, they will be mostly conducted with the galvo mirror. It is important to note that during this alignment, any time the collar and galvo are adjusted, the focus (micrometer above the emission objective) will need to be adjusted as well.

Using this protocol, we can see the four-dimensional dynamics of the TCRs on a T-cell surface (Figure 1, Movie 1). The main advantage of this microscope lies in the ability to track the visualized surface units of the TCRs, and to obtain quantified data from their size, motion, signal intensity, etc. (see Table of Materials). Movie 2 shows an example of the tracks obtained.

Discussion

The presented protocol was optimized for the usage of CD4⁺ T cells isolated from 5C.C7 transgenic mice on the LLSM instrument used, and therefore other cell systems and LLSMs may need to be optimized differently. However, this protocol shows the power of 4D imaging, as it can be used to quantify the dynamics of a surface receptor on an entire cell with the least distortion in physiological conditions. Therefore, there are many possible future applications of this technique.

A critical step is allowing the cells to settle at an appropriate concentration. If too many APCs settle on the coverslip and become too dense, it is hard to find a T cell that is interacting with only a single APC. When a T cell has multiple synapses, tracking and interpretation of data can become very complicated. Similarly, if too few APCs are present, finding a T cell forming a synapse is also difficult. In our hands, allowing 50,000 cells to settle for 10 min achieves an optimal density. However, this problem can be avoided if using a system with adherent cells. Cells can be grown in the incubator with the coverslips to a desired confluency.

Similarly, the number of T cells dropped into the system is dependent upon the size of the bath and the distance they can disperse. In the LLSM system used here, there is a 12 mL bath and a 2.5 mL bath, as opposed to the previous version of the system which only had a 10 mL bath available. We use the 12 mL bath for the original fluorescein imaging then switch to the 2.5 mL bath for imaging the cells. This allows for less thorough washing of the bath following the beam visualization step, and also lowers the number of T cells required for each imaging session. In turn, this would allow users to utilize fewer cells.

Finding cells at the correct point of interaction is also a challenge. In our hands, T cells take about 2 min to settle down to the APCs on the coverslip, so it is important to begin searching the coverslip for dynamic T cells close to APCs. A major improvement of this has been the recent addition of the LED light in the finder camera. If using a home-built system, we highly recommend including this feature in the design.

Finally, fluorescent labeling strategies are another important consideration. Each fluorescent protein or dye has a different quantum yield and rate of photobleaching. Fluorescent dyes are typically brighter, but if the cells have been stably transduced with a fluorescent protein labeled molecule, the label is replenished as the cell continues to produce the molecule. Therefore, labeling strategy is an important factor to consider when designing experiments.

We would like to conclude with a discussion on future directions for the technology. LLSM is also capable of structured illumination microscopy (SIM), which results in 150 nm XY resolution and 280 nm Z resolution, and is at least 10 times faster than widefield SIM¹². Therefore, while LLSM provides unprecedented speed of 4D imaging, it cannot achieve the spatial resolution of current super-resolution techniques^{4,5,6}. However, this resolution could be improved if a STED LLSM could be created. Light sheet STED and stimulated emission depletion with selective plane illumination microscopy (STED-SPIM) have been utilized, but lack the temporal resolution of LLSM^{21,22,23,24}. If STED-SPIM were adapted to incorporate a lattice, we could potentially obtain 50 nm axial resolution with far less photobleaching, and image faster than currently available techniques. Nevertheless, with current available technologies, LLSM gives us the fastest temporal resolution with high axial resolution.

Supplementary Material

Refer to Web version on PubMed Central for supplementary material.

Acknowledgments

We would like to acknowledge the advice and guidance from Dr. Vytas Bindokas at the University of Chicago. We thank the Integrated Light Microscopy Core Facility at the University of Chicago for supporting and maintaining the lattice light-sheet microscope. This work was supported by NIH New Innovator Award 1DP2AI144245 and NSF Career Award 1653782 (To J.H.). J.R. is supported by the NSF Graduate Research Fellowships Program.

References

1. Poulter NS, Pitkeathly WTE, Smith PJ, Rappoport JZ The Physical Basis of Total Internal Reflection Fluorescence (TIRF) Microscopy and Its Cellular Applications. *Methods in Molecular Biology* (Clifton, N.J.). 1251, 1–23, (2015).
2. Mattheyses AL, Simon SM, Rappoport JZ Imaging with total internal reflection fluorescence microscopy for the cell biologist. *Journal of Cell Science*. 123 (Pt 21), 3621–8, (2010). [PubMed: 20971701]
3. Axelrod D. Chapter 7 Total Internal Reflection Fluorescence Microscopy. *Methods in Cell Biology*. 89, 169–221, (2008). [PubMed: 19118676]
4. Rust MJ, Bates M, Zhuang X. Sub-diffraction-limit imaging by stochastic optical reconstruction microscopy (STORM). *Nature Methods*. 3 (10), 793–796, (2006). [PubMed: 16896339]
5. Betzig E, et al. Imaging Intracellular Fluorescent Proteins at Nanometer Resolution. *Science*. 313 (5793), 1642–1645, (2006). [PubMed: 16902090]
6. Hell SW, Wichmann J. Breaking the diffraction resolution limit by stimulated emission: stimulated-emission-depletion fluorescence microscopy. *Optics Letters*. 19 (11), 780, (1994). [PubMed: 19844443]
7. Shroff H, White H, Betzig E. Photoactivated Localization Microscopy (PALM) of Adhesion Complexes. *Current Protocols in Cell Biology*. 58 (1), 4.21.1–4.21.28, (2013).
8. Liu Z, Lavis LD, Betzig E. Imaging Live-Cell Dynamics and Structure at the Single-Molecule Level. *Molecular Cell*. 58 (4), 644–659, (2015). [PubMed: 26000849]
9. Ji N, Shroff H, Zhong H, Betzig E. Advances in the speed and resolution of light microscopy. *Current Opinion in Neurobiology*. 18 (6), 605–616, (2008). [PubMed: 19375302]
10. Erni R, Rossell MD, Kisielowski C, Dahmen U. Atomic Resolution Imaging with a sub-50 pm Electron Probe. <https://escholarship.org/uc/item/3cs0m4vr> (2019).
11. Kizilyaprak C, Daraspe J, Humbel BM Focused ion beam scanning electron microscopy in biology. *Journal of Microscopy*. 254 (3), 109–114, (2014). [PubMed: 24707797]
12. Chen BC, et al. Lattice light-sheet microscopy: Imaging molecules to embryos at high spatiotemporal resolution. *Science*. (2014).
13. Ni J, et al. Adoptively transferred natural killer cells maintain long-term antitumor activity by epigenetic imprinting and CD4+ T cell help. *Oncoimmunology*. 5 (9), e1219009, (2016).
14. Chaudhri A, Xiao Y, Klee AN, Wang X, Zhu B, Freeman GJ PD-L1 Binds to B7-1 Only In Cis on the Same Cell Surface. *Cancer Immunology Research*. 6 (8), 921–929, (2018). [PubMed: 29871885]
15. Forbes CA, Scalzo AA, Degli-Esposti MA, Coudert JD Ly49C-dependent control of MCMV Infection by NK cells is cis-regulated by MHC Class I molecules. *PLoS pathogens*. 10 (5), e1004161, (2014).
16. Schöneberg J, et al. 4D cell biology: big data image analytics and lattice light-sheet imaging reveal dynamics of clathrin-mediated endocytosis in stem cell-derived intestinal organoids. *Molecular biology of the cell*. 29 (24), 2959–2968, (2018). [PubMed: 30188768]
17. Gao R, et al. Cortical column and whole-brain imaging with molecular contrast and nanoscale resolution. *Science (New York, N.Y.)*. 363 (6424), eaau8302, (2019).
18. Cai E, et al. Visualizing dynamic microvillar search and stabilization during ligand detection by T cells. *Science (New York, N.Y.)*. 356 (6338), eaal3118, (2017).
19. Ritter AT, et al. Actin Depletion Initiates Events Leading to Granule Secretion at the Immunological Synapse. *Immunity*. (2015).

20. Lim JF, Berger H, Su I-H Isolation and Activation of Murine Lymphocytes. *Journal of visualized experiments: JoVE*. (116), (2016).
21. Huang J, et al. A Single Peptide-Major Histocompatibility Complex Ligand Triggers Digital Cytokine Secretion in CD4+ T Cells. *Immunity*. 39 (5), 846–857, (2013). [PubMed: 24120362]
22. Irvine DJ, Purbhoo MA, Krogsgaard M, Davis MM Direct observation of ligand recognition by T cells. *Nature*. 419 (6909), 845–849, (2002). [PubMed: 12397360]
23. Jansson A. A mathematical framework for analyzing T cell receptor scanning of peptides. *Biophysical journal*. 99 (9), 2717–25, (2010). [PubMed: 21044568]
24. Mickoleit M, et al. High-resolution reconstruction of the beating zebrafish heart. *Nature Methods*. 11 (9), 919–922, (2014). [PubMed: 25042787]

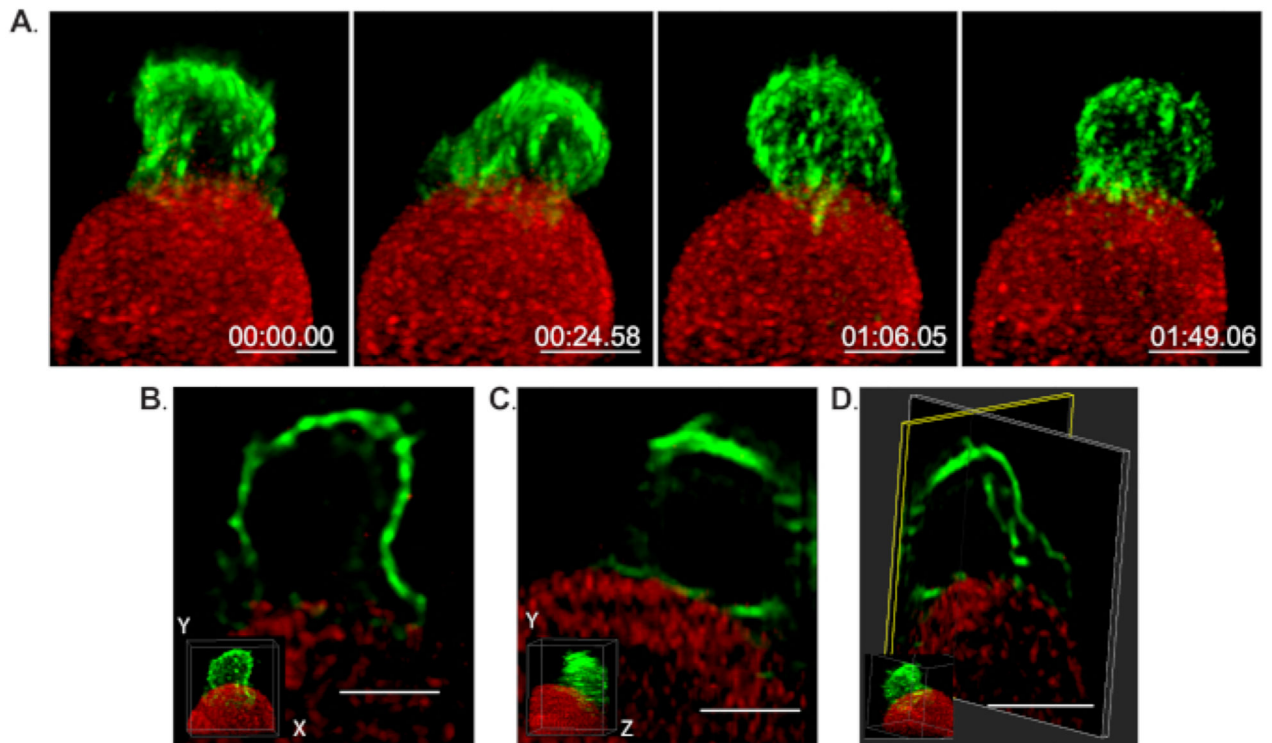


Figure 1: 4-dimensional imaging of T cell-APC Synapse.

(A) A representative example 3D time-lapse LLSM images showing a T cell interacting with an APC. Shown are the TCR (green, labeled by anti-TCR-AF488) dynamics in recognizing antigens presented on the surface of an APC (red, cytosolic mCherry). Scale bar = 5 μm .

Also see Movie 1. (B) Orthogonal XY slice of (A). Inset is a reference frame of a whole cell. Scale bar = 5 μm .

(C) Orthogonal YZ slice of (A). Inset is a reference frame of a whole cell. Scale bar = 5 μm .

(D) Dual orthogonal slice of (A). Inset is reference frame of whole cell. Scale bar = 5 μm .

Also see Movie 3. Please click [here](#) to view a larger version of this figure.

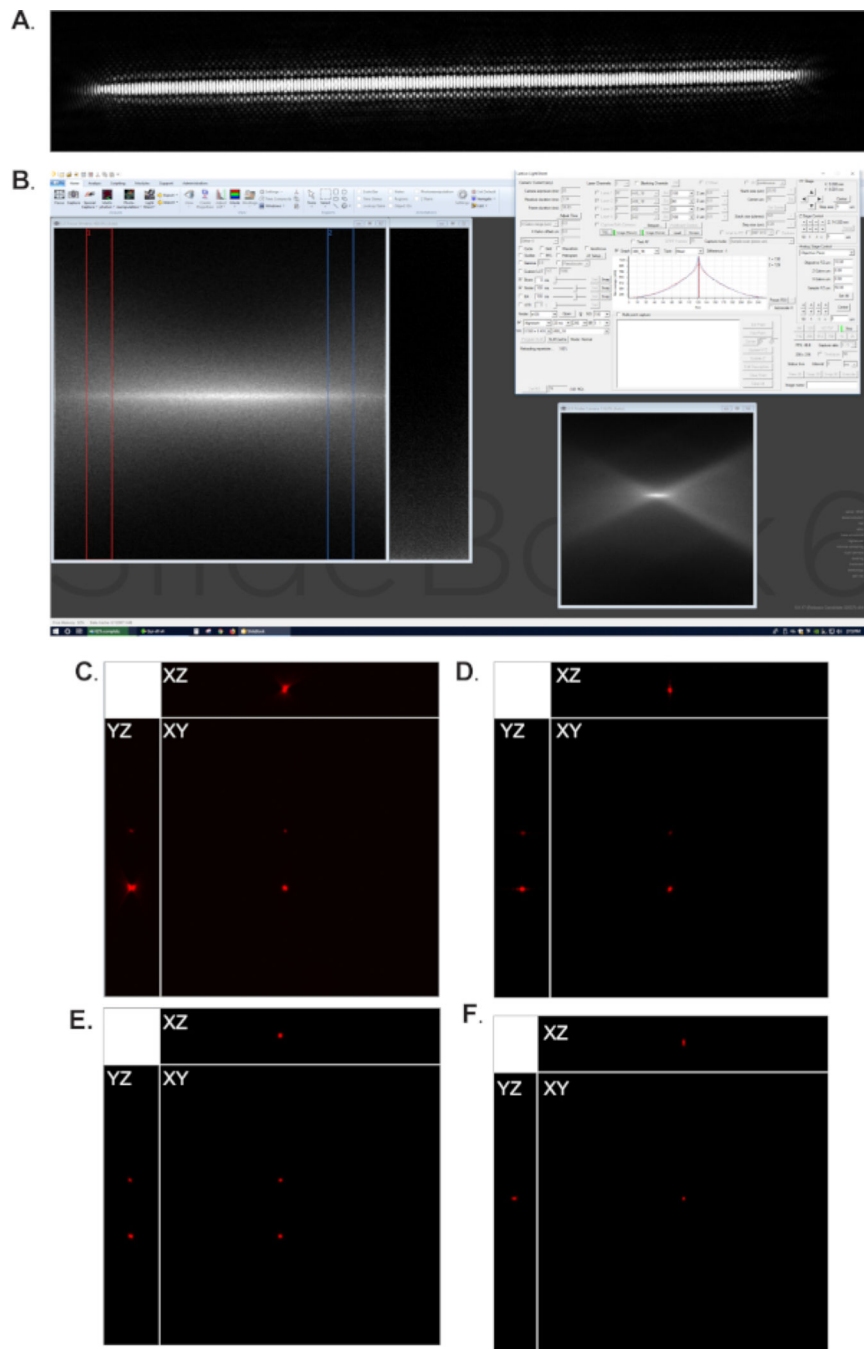


Figure 2: LLSM alignment.

(A) Desired beam pattern for LLSM imaging experiment. (B) Screenshot of the beam alignment process; on the left is the focus window showing the narrowed, focused beam; at the top right is a graph showing that the beam is centered within the window; at the bottom right is the finder camera, which should also be a thin, focused beam. (C) Maximum intensity projections (MIPs) of a bead by objective scan. (D) Maximum intensity projections (MIPs) of a bead by z-galvo scan. (E) Maximum intensity projections (MIPs) of a bead by z

+objective scan. **(F)** Maximum intensity projections (MIPs) of a bead by sample scan.
Please click here to view a larger version of this figure.

Author Manuscript

Author Manuscript

Author Manuscript

Author Manuscript